SPACE HARMONIC ANALYSIS OF MAGNETIC FIELDS IN A COMPENSATED PULSED ALTERNATOR OR AN ACTIVE ROTARY FLUX COMPRESSOR

Jayesh A. Parekh, W. L. Bird, A. C. Patel, and H. H. Woodson

Center for Electromechanics
The University of Texas at Austin
Taylor Hall 167
Austin, Texas 78712

Summary

This paper discusses the space harmonic Fourier analysis of magnetic fields for a compensated pulsed alternator (compulsator) or an active rotary flux compressor (ARFC), which has been applied for two particular sets of boundary conditions appropriate for these machines to calculate magnetic field distributions, inductances, and how those inductances vary with rotor position. The results of the analytic model are compared with experimental results. This paper also shows the results of the extensive parametric studies using the inductances calculated from space harmonic distribution (SHD) code to explore design alternatives to improve the performance of these machines.

Introduction

The operation of a compensated pulsed alternator (compulsator) or an active rotary flux compressor (ARFC) involves a number of phenomena, the most important of which is the delivery of output current through a circuit of varying inductance that provides:

a. compensation to reduce inductive impedance to current flow, and
b. flux compression by changing inductance to enhance output voltage.

Because the operation depends intimately on the magnetic fields in the machine and how they vary in time and space, it is important to have as accurate a magnetic field analysis as practical. The basic problem thus becomes one of calculating inductance as a function of rotor position.

Both the armature winding and the compensating winding occupy known radial and azimuthal regions in the air gap.

A solution of Laplace's equation for a two-dimensional problem in cylindrical coordinates with radial and azimuthal variations is a sinusoid; hence if the excitation and boundary conditions can be expressed as Fourier series, then the fields in the machine can be found as space Fourier series.

Fields and Stored Magnetic Energy

The machine geometry to be analyzed is shown in Figure 1. The origin $(\psi - \alpha) = o$ corresponds to the center line of the belt of the windings that has a missing conductor, which is the result of the serpentine winding configuration. Both armature and compensating windings are shown as occupying certain radial and azimuthal regions defined by the angles and radii. If, at a particular radius in one of the windings, we plot the current density as a function of angle, we get the current distribution shown in Figure 2. Thus, assuming a series of the form

$$J = J_o + \sum_{n=1}^{\infty} J_n \cos n (\psi - \alpha), \qquad (1)$$

the coefficients are found in the usual way.

Using the radial variable ρ to denote a location within a current distribution and considering the interior of the machine where the conductors carry current axially and end effects can be neglected, a differential element of the current density can be treated as an axial (z - directed) current sheet, which for the n^{th} component is

$$\overline{K}_n = \overline{A}_z K_n \cos n (\psi - \alpha) \qquad (2)$$

where $K_n = J_n \, d\rho$.

Field Intensities

The next step is to find the field produced in the

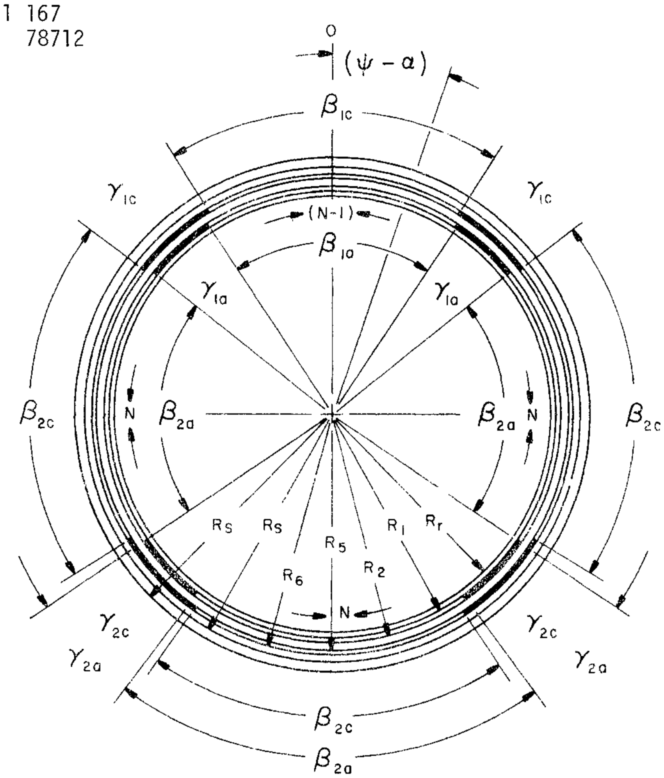

Fig. 1. Geometry of the machine used for space harmonic distribution inductance calculation

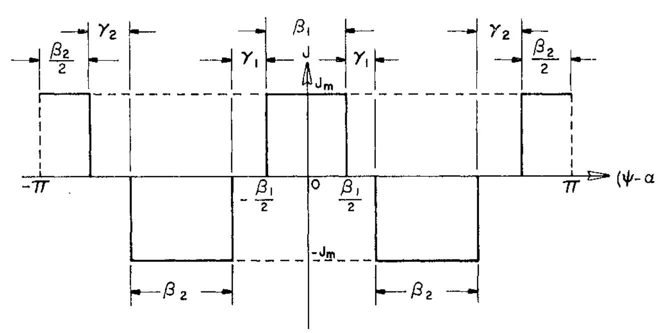

Fig. 2. Developed view of compulsator winding current sheets

Report Documentation Page

Form Approved
OMB No. 0704-0188

1. REPORT DATE	2. REPORT TYPE	3. DATES COVERED
JUN 1981	**N/A**	**-**

4. TITLE AND SUBTITLE
Space Harmonic Analysis Of Magnetic Fields In A Compensated Pulsed Alternator Or An Active Rotary Flux Compressor

5a. CONTRACT NUMBER
5b. GRANT NUMBER
5c. PROGRAM ELEMENT NUMBER

6. AUTHOR(S)

5d. PROJECT NUMBER
5e. TASK NUMBER
5f. WORK UNIT NUMBER

7. PERFORMING ORGANIZATION NAME(S) AND ADDRESS(ES)
Center for Electromechanics The University of Texas at Austin Taylor Hall 167 Austin, Texas 78712

8. PERFORMING ORGANIZATION REPORT NUMBER

9. SPONSORING/MONITORING AGENCY NAME(S) AND ADDRESS(ES)

10. SPONSOR/MONITOR'S ACRONYM(S)

11. SPONSOR/MONITOR'S REPORT NUMBER(S)

12. DISTRIBUTION/AVAILABILITY STATEMENT
Approved for public release, distribution unlimited

13. SUPPLEMENTARY NOTES
See also ADM002371. 2013 IEEE Pulsed Power Conference, Digest of Technical Papers 1976-2013, and Abstracts of the 2013 IEEE International Conference on Plasma Science. Held in San Francisco, CA on 16-21 June 2013. U.S. Government or Federal Purpose Rights License.

14. ABSTRACT

15. SUBJECT TERMS

16. SECURITY CLASSIFICATION OF:			17. LIMITATION OF ABSTRACT	18. NUMBER OF PAGES	19a. NAME OF RESPONSIBLE PERSON
a. REPORT	b. ABSTRACT	c. THIS PAGE			
unclassified	**unclassified**	**unclassified**	**SAR**	**4**	

Standard Form 298 (Rev. 8-98)
Prescribed by ANSI Std Z39-18

machine by the current sheet of Equation 2 for each winding and then integrate over both winding distributions to find the total field strength. Because this is a linear field problem, each Fourier component for each winding can be considered separately and then the results may be summed later.

To proceed with the analysis we consider only a current sheet described by equation 2 in an air gap with free-space permeability μ_0. Except within the current sheet, which is infinitesimal ($d\rho$) in thickness, and possibly at the boundaries, there are no currents flowing, in which case

$$\nabla \times \bar{H} = 0, \tag{3}$$

which allows $\bar{H}$ to be described as

$$\bar{H} = -\nabla U. \tag{4}$$

Because

$$\bar{B} = \mu_0 \bar{H} \tag{5}$$

and

$$\nabla \cdot \bar{B} = 0 \tag{6}$$

the potential U must be a solution of Laplace's equation

$$\nabla^2 U = 0 . \tag{7}$$

In the interior of the machine axial variations of fields can be ignored; thus Laplace's equation for cylindrical coordinates can be written with $\frac{\partial}{\partial z} = 0$ to obtain

$$\nabla^2 U = \frac{1}{r}\frac{\partial}{\partial r}\left(r\frac{\partial U}{\partial r}\right) + \frac{1}{r^2}\frac{\partial^2 U}{\partial \theta^2} = 0. \tag{8}$$

The variables can then be separated by assuming a product solution

$$U = R(r)\,\Theta(\theta) \tag{9}$$

substituting it in Equation 8 and solving the two resulting differential equations to obtain the general solution

$$U_n = \left(C r^n + D r^{-n}\right)\left(A \sin n\theta + B \cos n\theta\right). \tag{10}$$

For the general current sheet of Equation 2, which is located at $r = \rho$, two regions are identified:

region i: $R_r < r < \rho$ $\left\{\right.$The field is calculated at a point radially inwards from the current sheet.

region o: $\rho < r < R_s$ $\left\{\right.$The field is calculated at a point radially outward from the current sheet.

Subscripts i and o will be used to denote the region, with respect to the current sheet, in which the field is being calculated.

The two sets of boundary conditions for a compulsator or an ARFC are shown in Table I. Both boundary conditions I and II are for a laminated rotor made of ferromagnetic material of high permeability. Boundary condition I pertains to solid steel poles whereas boundary condition II pertains to laminated stator magnetic material.

The application of these two sets of boundary conditions and the resulting field expressions are shown in detail in references 1 and 2.

TABLE I
Two Sets of Compulsator-ARFC Boundary Conditions

At Radius	Boundary Condition I	Boundary Condition II
Rotor Surface $r = R_r$	Infinitely permeable $H_{\theta i} = 0$	
Stator Surface $r = R_s$	Perfectly Conducting $H_{ro} = 0$	Infinitely Conducting $H_{\theta o} = 0$
At Current Sheet $r = \rho$	H_r continuous $H_{ri} = H_{ro}$	
At Current Sheet $r = \rho$	$\left(H_{\theta no} - H_{\theta ni}\right) = K_n \cos n(\theta - \alpha)$	

To calculate the total field due to single winding consider first the compensating winding which, according to Figure 1, occupies the radial space

$$R_5 < \rho < R_6.$$

For this winding three regions are identified in which the field must be calculated separately as follows:

$$\text{for } R_r < r < R_5 \quad H_{nc} = \int_{R_5}^{R_6} d\,H_{nic} \tag{11}$$

$$\text{for } R_5 < r < R_6 \quad H_{nc} = \int_{R_5}^{r} d\,H_{noc} + \int_{r}^{R_6} d\,H_{nic} \tag{12}$$

$$\text{for } R_6 < r < R_s \quad H_{nc} = \int_{R_5}^{R_6} d\,H_{noc}. \tag{13}$$

The use of these integrals leads to the field expressions for the compensating winding. Because the process is exactly the same for the armature winding, the field expressions for the armature winding are obtained from those for the compensating windings by making the replacements:

$$J_{nc} \Rightarrow J_{na} \qquad R_6 \Rightarrow R_1$$

$$\alpha_c \Rightarrow \alpha_a \qquad R_5 \Rightarrow R_2$$

References 1 and 2 contain these final field expressions for the two sets of boundary conditions.

Magnetic Stored Energies

The next step in this space harmonic field analysis is to use the field intensities to calculate the stored magnetic energy and from that the self and mutual inductances of the windings. Basically the magnetic stored energy is calculated from

$$W_m = \int_{vol} \frac{1}{2}\mu_0 H^2 \; d\,vol. \tag{14}$$

It will be convenient to calculate the self- and mutual inductances separately. For either winding

$$W_m = \int_0^{2\pi} \int 1/2\ \mu_0(H_r^2 + H_\theta^2)\ell r\ dr\ d\theta. \tag{15}$$

Because different harmonics are orthogonal with respect to the integration on θ, all cross terms will integrate to zero and Equation 15 can be written as

$$W_m = \sum_{n=1}^{\infty} W_{mn} \tag{16}$$

with

$$W_{mn} = \int_0^{2\pi}\int 1/2\ \mu_0(H_{rn}^2 + H_{\theta n}^2)\ell r\ dr\ d\theta. \tag{17}$$

Each field component can be written in the form

$$H_{rn} = H_{rnm} \sin n(\theta-\alpha) \tag{18}$$

$$H_{\theta n} = H_{\theta nm} \cos n(\theta-\alpha). \tag{19}$$

Squaring these expressions, replacing the squares of the sinusoidal functions with trigonometric identities, and carrying out the integration on θ yields zero for the sinusoidal terms leaving

$$W_{mn} = \frac{\pi\mu_0\ell}{2}\int (H_{rnm}^2 + H_{\theta nm}^2) r dr. \tag{20}$$

Using the field expressions, the stored energies for the various regions for armature and compensating winding excited separately were calculated. The resulting expressions are tabulated and displayed in references 1 and 2.

Using the fact that for self-inductance

$$W_m = 1/2\ Li^2 \tag{21}$$

and the expressions for energies, along with the relations for the maximum compensating and armature winding current densities yields the self-inductance for use in the expression

$$L = \sum_{n=1}^{\infty} L_n. \tag{22}$$

The final calculation to be made is of the mutual inductance between the armature and compensating windings. This requires the calculation of magnetic stored energy resulting only from simultaneous excitation of both windings. From Equation 15 these cross terms yield

$$W_m = \int_0^{2\pi}\int \mu_0(H_{rc}H_{ra} + H_{\theta c}H_{\theta a})\ell r\ dr\ d\theta. \tag{23}$$

Using the orthogonality of different Fourier components and the general form of the field expressions given in Equations 18 and 19 with the nth component along with the use of trigonometric identities on the products of the sinusoidal functions and integrating on θ yields

$$W_{mn} = \pi\mu_0\ell\int (H_{rnmc}H_{rnma} + H_{\theta nmc}H_{\theta nma})\cos n(\alpha_a-\alpha_c) r dr. \tag{24}$$

The use of the field expressions with this equation results in the mutual energy storage expressions in the five regions. Combining these energy expressions with the maximum compensating and armature winding current density expressions, the expression

$$W_{mn} = M_n i_c i_a \tag{25}$$

and

$$M = \sum_{n=1}^{\infty} M_n \cos n(\alpha_a-\alpha_c) \tag{26}$$

yields

$$n \neq 2 \qquad M_n = \sum_{k=1}^{5} \frac{W_{mnk}}{i_a i_c} \tag{27}$$

$$n = 2 \qquad M_n = \sum_{k=1}^{5} \frac{W_{m2k}}{i_a i_c} \tag{28}$$

When the armature and compensating windings are connected in series, the total inductance of the circuit is

$$L = L_a + L_c + 2M \tag{29}$$

which with the use of Equation 26 becomes

$$L = L_a + L_c + 2\sum_{n=1}^{\infty} M_n \cos n(\alpha_a-\alpha_c) \tag{30}$$

which describes explicitly how the circuit inductance varies with the relative angular position $(\alpha_a-\alpha_c)$ of the two windings.

Compulsator-ARFC Inductance

The calculated magnetic field strengths, magnetic energy, and effective inductance for the two sets of boundary conditions were used to develop computer programs called space harmonic distribution (SHD) codes. Two machines that match our first set of boundary conditions, viz, laminated rotor and solid stator poles, had been designed and fabricated at the Center for Electromechanics at the University of Texas at Austin (CEM-UT). These were the engineering prototype compulsator[1] and the desk model compulsator[3]. The second set of boundary conditions, viz, laminated rotor and laminated stator, was an attempt to increase the magnetic flux compression ratio of a compulsator or an ARFC. An ARFC was designed and fabricated with laminated rotor and laminated stator at CEM-UT.[4] The optimum angular span for the windings and conductor configuration were selected with the help of the SHD code corresponding to boundary condition II.[2] The exact winding configuration and system geometry of the three machines were readily available to use in calculating the effective inductance of each machine. For boundary condition I, since the poles are not perfect conductors there will be some penetration of the field into the pole region. An effective $H_r = 0$ boundary (assuming $\mu = \mu_0$ in the region between R_s and R_s') was located at a certain depth into the pole which yielded SHD code results that matched the measured values. The calculated and measured values of effective minimum and maximum inductance of the three machines are given in Table II.

In using the SHD code the effect of the end turns on the calculated inductance per unit length must be considered unless the machine has many poles, in which case the length of the end turns is small compared to the active length of the rotor.

Parametric Design Studies

The two SHD codes for the two sets of boundary conditions were used to study the variation in inductance as different parameters are changed in the engineering prototype compulsator and the ARFC. Only the parametric design study for the prototype compulsator will be discussed here. The parametric design study for the ARFC is discussed in detail in reference 2.

TABLE II
Calculated and Measured
(LCR bridge measurement at 1.0 kHz)
values of effective minimum and maximum inductance (H)

Machine	L_{max}		L_{min}		Flux compression ratio	
	calc	meas	calc	meas	calc	meas
Prototype compulsator	177.7μ	176μ	24.1μ	26.3μ	7.37	6.69
Desk model compulsator	138μ	136μ	16.4μ	17.5μ	8.39	7.77
ARFC	1.19m	1.09m	26.4μ	23.2μ	45.08	46.98

Self-Inductance vs. Radial Position of the Winding

To determine the sensitivity of the self-inductance of the armature winding to the inner radius of the winding the SHD code was suitably modified and the calculations for the prototype compulsator were repeated over the range $R_r \leq R_1 \leq R_s - (R_2 - R_1)$. The self-inductance of the armature winding varied from 80μH to 10μH as the inner radius of the armature winding was increased from the rotor surface until the outer radius coincided with the pole faces.

Effective Inductance vs. Radial Separation of Windings

The flux compression ratio decreases significantly as the radial separation $(R_5 - R_2)$ is increased To achieve a narrower pulse width it is necessary to operate the device at the smallest air gap that mechanical and electrical constraints will allow.

Effective Inductance vs. Circumferential Span of Windings

The circumferential distribution of the windings is important in determining the effective inductance as a function of the angular position of the rotor winding relative to the compensating winding during the pulse. The calculated values of (L_{max}/L_{min}) are plotted against compensating winding conductor span at N=12 turns (β_{2c}) in Figure 3. The radial thickness of the windings is assumed to remain constant.

To maintain the same winding resistance the same variation of conductor span is considered but with a constant conductor cross-section. Flux compression ratio decreases as the conductor span is reduced for the constant cross-section case. Thus a wide, radially thin conductor design is preferable for maximum compression ratio.

Number of Poles

The pulse width of the discharge can be decreased by increasing the number of poles. But as shown in Figure 4 the flux compression ratio decreases with increasing number of poles.

Conclusions

The detailed space harmonic analysis described in this paper enabled the successful establishment of expressions for fields, stored energy and inductances that agree well with measurements from three experimental models. The analytic model provides a versatile tool for parametric-design studies of both a compulsator and an ARFC. The corresponding SHD code facilitates the calculation of the space harmonic current densities, magnetic stored energies, self- and mutual inductances, and the flux compression ratio. Over and above proving the viability of the compulsator concept, the SHD technique for calculating effective inductances is a useful design tool.

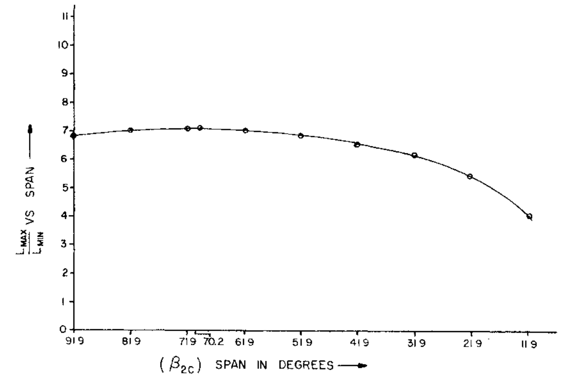

Fig. 3. Flux compression ratio of the prototype compulsator versus conductor span--constant radial thickness

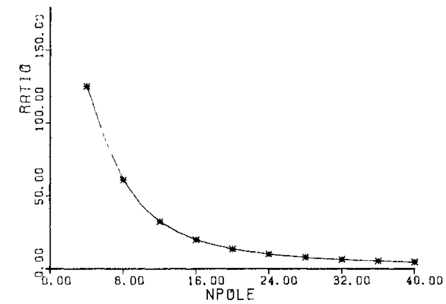

Fig. 4. Flux compression ratio vs. number of poles in a 1-m diameter laminated rotor, laminated stator ARFC

References

1. Jayesh A. Parekh, "Space Harmonic Analysis of Magnetic Fields in a Compensated Pulsed Alternator," Master's thesis, the University of Texas at Austin, May 1980.

2. Ankil C. Patel, "Space Harmonic Analysis of Magnetic Fields in a Rotary Flux Compressor," Master's thesis, the University of Texas at Austin, August 1981.

3. Mark Pichot, "Design, Construction, and Testing of a Desk Model Compensated Pulsed Alternator," Master's thesis, the University of Texas at Austin, May 1980.

4. M. L. Spann, "The Design, Assembly, and Testing of an Active Rotary Flux Compressor," proceedings of this conference.

This work was supported by the Texas Atomic Energy Research Foundation and Lawrence Livermore National Laboratory.